Current Trends in Biotechnology and Pharmacy
Vol. 19(3) 2462-2479, July 2025, ISSN 0973-8916 (Print), 2230-7303 (Online)
DOI: 10.5530/ctbp.2025.3.30

Exploring the Anti-Hepatocarcinogenic Efficacy of *Launaea sarmentosa* in NDEA-Induced Wister Albino Rats

Soumya Kiran Mishra[1], Roja Sahu[1],*, Prafulla Kumar Sahu[1,2,*], Kota Padmaja[3], K.A. Chowdary[4]

[1]School of Pharmacy, Centurion University of Technology and Management, Odisha, India-767001
[2]Department of Pharmacy, Keonjhar Institute of Medical Science and Research, Keonjhar, Odisha, India
[3]Raghu College of Pharmacy, Dakamarri, Bheemunipatnam (M), Visakhapatnam, Andhra Pradesh, India-531162
[4]Royal College of Pharmacy and Health Sciences, Berhampur, Odisha, India

***Corresponding Author**: kunasahu1@gmail.com

Abstract

Launaea sarmentosa (Asteraceae) rich in alkaloids, flavonoids and glycosides has traditionally popular therapeutic virtues, particularly in treating cancer. This work was aimed to assess the anticancer efficacy of aerial part of *Launaea sarmentosa* extracted with ethanol (EELS) against hepatocellular carcinoma (HCC) induced by N-Nitrosodiethylamine (NDEA)+phenobarbital+CCl_4 in Wister albino rats. Firstly, pharmacognostical parameters of the plant was established followed by *in vitro* antioxidant studies. Successively, *in vitro* and *in vivo* anticancer survey of EELS (100, 200 and 400 mg/kg) was performed correspondingly in HepG2 cells and NDEA-induced HCC in Wister albino rats along with detailed biochemical, morphological and histopathological assessment. EELS administration (14 days) reinstated the altered body weight to normalcy and prevented subsequent rise of liver weight as a prognostic marker in HCC. The *in vitro* study presented promising antioxidant action of EELS correlating with *in vivo* results (enzymatic, non-enzymatic antioxidants and lipid peroxidation). A remarkable reduction in hepatic biomarkers (ALP, ALT, and AST) as well as inflammatory biomarkers (IL-1β and TNF-α) were observed in EELS-treated animals in a concentration-dependent manner. Finally, histopathological investigation of the liver tissue showed restoration of typical tissue skeleton along with reduced expression of proliferative markers on EELS administration as compared to untreated HCC animals. Outcome of this experiment have established anti-hepatocarcinogenic capacity of EELS, thereby advocating its use along with conventional therapies for HCC.

Keywords: *Launaea sarmentosa*, hepatocellular carcinoma, Anti-oxidant, hepatic biomarkers, inflammatory biomarkers, hepatic biomarkers

Introduction

Hepatocellular carcinoma (HCC) is a major contributor to cancer-related mortality (survival rate of below 9%) (1,2) with a prevalence that is three times higher in males compared to females on a global scale (3), accounting for 830,000 deaths in 2020, followed by lung and colon cancer (4). It exhibited resistance to chemotherapy with moderate efficacy towards radiotherapy, thereby restricting the choices of medication in case of an inoperable tumor. This opens new avenues for alternative therapies using natural compounds or their secondary metabolites with proven anti-carcinogenic and hepatoprotective action (5). Medicinal plants have demonstrated their worth as reservoirs of compounds with therapeutic potential and continue to be a significant source for discovering novel drug candidates (6). In addition,

Current Trends in Biotechnology and Pharmacy
Vol. 19(3) 2462-2479, July 2025, ISSN 0973-8916 (Print), 2230-7303 (Online)
DOI: 10.5530/ctbp.2025.3.30

herbal medications are currently the subject of substantial scientific attention due to their ability to supply essential biomolecules for treating many diseases including cancer, while also offering a wide range of long-term usage and safety. Hundreds of medicinal plants are being employed as a treatment modality either directly or indirectly by derivatising various synthetic molecules (7). The discovery of plant-derived drugs has led to the development of over 120 single-entity drugs used in western medicine, including established drugs such as atropine, codeine, colchicine, pilocarpine, and quinine, as well as newer drugs like galanthamine and paclitaxel (8-10). It should come as no surprise that numerous powerful chemotherapeutic agents, including taxol, doxorubicin, topotecan, cisplatin, vincristine, vinblastine and vindesine were extracted from the plants (5). The present focus on alternative medicine necessitates an extensive effort to develop new chemicals that can assist in liver cancer treatment while minimizing adverse effects.

Pharmacognosy, together with ethnobotany, pharmacology, and biological sciences, plays a crucial role in guaranteeing the quality control of ethnomedicinal remedies (11). The ongoing Pharmacognostical investigation examines roots, leaves, and petioles of the plant. It encompasses inspection, detailed interpretation and documentation. In addition, high-resolution pictures were taken to ensure an accurate evaluation. The ethnomedicinal study has moved forward with recent advancements in the pharmacognostical profiling of plants (12,13). Herbal medications must be pharmacognostically evaluated to avoid the inclusion of inferior components and sometimes whole product substitution, thereby validating standard potency, purity and therapeutic value (14-16). Therefore, the objective of this work was to examine the pharmacognostic characteristics of L. sarmentosa and investigate the potential of EELS as an anti-carcinogenic agent against NDEA-induced HCC.

Launaea sarmentosa (*L. sarmentosa*) or “Sagar Paathri” is a costal sand dunes, runners well grown in the western zones of India belongs to family Asteraceae (17,18). The plant bears yellow flower heads with milky white latex (19), traditionally used for the treatment of diarrhea (20). *L. sarmentosa* is widely known for its antihelminthic activity, wound healing activity (21,22), thrombolytic and membrane stabilizing activity (23), antimicrobial activity (24,25), analgesic, anti-pyretic (26) and anti-inflammatory activity (27), alpha glucosidase inhibitory activity and antioxidant activity (28). Such activity may be attributed by the presence of a variety of phytoconstituents including alkaloids, carbohydrates, amino acids, steroids, glycosides, flavonoids, etc in it (29). *L. sarmentosa* roots are rich in α and β amyrin acetate, lupeol acetate and psi taraksa sterol acetate, 4-allyl-2,6-dimethoxyphenol glucopyranoside, scorzoside, ixerisoside D, and 9α-hydroxypinoresinol (30,31). Many species of Launaea including *Launaea nudicaulis* is proven to possess cytotoxic potential against HePG-2 and PC3 cancer cells (32).

Due to their radical scavenging and antioxidant properties, flavonoids and other polyphenolic substances can prevent cancer growth (33). The presence of life-sustaining phytoconstituents has prompted researchers to extensively study phytotherapy, which has led to natural products becoming alternative medicine or functional foods to combat carcinogens (34). Thus, in our study, we have primarily focused on assessing anti-cancer potential of ethanolic extract of aerial part of *Launaea sarmentosa* (EELS) against N-Nitrosodiethylamine (NDEA) induced HCC in Wister albino rats.

Materials and Methods

Chemical and reagents required

Analytical-grade chemicals and reagents, including acetone, methanol, ethanol, hydrochloric acid, Mayer’s reagent, ferric chloride, Fehling solutions A and B, chloroform, sulfuric acid, ammonia, glacial acetic acid, dimethyl sulfoxide (DMSO), sodium dihydrogen phosphate, disodium hydrogen phosphate,

hydrogen phosphate, ascorbic acid, 1,1-diphenyl-2-picrylhydrazyl (DPPH), sodium nitroprusside, sulfanilamide, naphthyl ethylene diamine hydrochloride, and phosphoric acid, were obtained from Finar Scientific Chemicals, Mumbai, Maharashtra.

Collection of plant materials and authentication

Plant samples of L. sarmentosa were gathered in October 2022 from the rocks of the seashore of Visakhapatnam. L. Rasingam, the Scientist In-Charge of the Botanical Survey of India in Hyderabad, Telangana, identified and verified the samples. A voucher specimen (BSI/DRC/2022-23/Identification/438) has been stored in the Botanical Survey of India, Hyderabad, herbarium department for future reference.

Extraction procedure

Following their collection, aerial portions of L. sarmentosa were dried under shade and crushed into fine powder. Nearly 1.5 kg of this powder was subjected to Soxhlet extraction for 48-72 hours using ethanol as the solvent and then dried using a rotary evaporator (model-R-1001-VN, ZGSIT, China) (35).

Pharmacognostic evaluation

The microscopic examination was performed on the transverse sections (root, petiole and leaf) of the FAA fixed sample following safranin staining using Axiolab 5 trinocular bright field microscope attached to Zeiss Axiocam208 color digital camera. Furthermore, quantitative microscopy (epidermal number, stomatal index, stomatal number, vein islet number, palisade ratio and vein termination number) and powdered characteristics of the drug was examined through trinocular microscope (Olympus BX43 and Nikon ECLIPSE E200) connected to digital camera (Zeiss ERc5s) following the method of (36). In addition, preliminary evaluations were conducted on EELS to assess the presence of phytochemicals (37).

In-vitro assessment of antioxidant potential

Scavenging activity of EELS (10-50 µg/ml) on Hydrogen peroxide (H_2O_2), Nitric oxide (NO) (38) and 2,2-diphenyl-1-picrylhydrazyl (DPPH) (36,39) radical was estimated through a UV–Vis double beam spctrophotometer (UV-1900i, Shimadzu, Japan) by taking ascorbic acid as control. The percentage scavenging is assessed as follows:

$$\%\, Scavenging\ activity = \frac{A_b - A_t}{A_b} \times 100 \quad \text{..... (Eq. 1)}$$

where A_t: absorbance of test or standard and A_b: absorbance of blank.

The percentage scavenging activity (Y-axis) was plotted against the concentration (X-axis). Furthermore, the resulting graph was extrapolated to ascertain the half maximal inhibitory dose (IC_{50} value) of the plant extract required to achieve 50% scavenging activity (40).

MTT assay

EELS was subjected to a cytotoxicity activity study using the MTT assay. HepG2 cell was cultured in 96-well plates for approximately 24h using 50% CO_2 at 37°C. The cells were initially distributed at a density of 10^4 cells per well and thereafter subjected to varying concentrations of extracts. The control group consisted of cells that had been treated with the desired solvent. Subsequently, the cells were treated with a solution of MTT (3-(4,5-dimethylthiazol-2-yl)-2,5-diphenyl tetrazolium bromide) at a concentration of 0.5 mg/ml, followed by the addition of the solvent above. The formazan generated was subsequently extracted from the MTT-containing media and dispersed in DMSO (200 µl), after which the optical density was measured. Percentage of HepG2 cell inhibition as per the formula given below (Eq. 2) (37).

$$\%Cell\ inhibition = \frac{OD\ of\ treated\ cells}{OD\ of\ control\ cells} \times 100 \quad \text{..... (Eq. 2)}$$

Acute Toxicity Study

This study was executed by administering various doses (5-2000 mg/kg) of EELS in male Swiss albino mice weighing 25-30 gm as directed in OECD 420 guidelines. The animals

were surveilled for 12h for any physiological and behavioural alterations, while mortality was documented for 24 hours. No death was reported in this 24h period in all treatment doses. Based on this pilot investigation, three doses (100mg/kg, 200mg/kg, and 400mg/kg) were chosen for future experiments.

Estimation of anticancer efficacy of EELS in hepatocellular carcinoma

Experimental animals

For this investigation, Wistar albino rats aged 50-55 days were procured from the National Institute of Nutrition in Hyderabad. Subjects were kept in polystyrene, properly ventilated enclosures at ambient temperature with a 12-hour light/dark cycle. All animals were fed a regular pelleted diet and given unrestricted access to food and water. Each study was conducted with the authorisation of the Institutional Animal Ethics Committee of the School of Pharmacy, Centurion University of Technology and Management, Odisha (1549/PO/Re/S/2011/CPCSEA), in accordance with the norms set by NIH and CPCSEA, India.

Tumor induction and experimental design

Induction of liver cancer in Wistar rats was performed using the method of Pound et al (41) and Yadav et al (42) with little modification as required (43). Precisely partial hepatectomy (PH) was first performed on the all the experimental animals. After 24 h of stabilization animals were administered with a single dose of NDEA (100 mg/kg b.w., i.p.). Following NDEA induction, phenobarbital sodium (PB; 0.05% w/v, P.O.) was provided in drinking water up to 4 weeks. Along with this CCl_4 (1 ml/kg b.w., s.c.) was administered to the animals twice a week for first two weeks.

Thirty animals were grouped into 5 sets each containing six rats. Group I (normal control) rats were provided with no treatment. Group II (NDEA) animals were treated with NDEA to induce HCC as described above and were devoid of any treatment. Groups III-V (treatment groups) animals with HCC were treated with EELS (100, 200 and 400 mg/kg b.w., p.o. respectively) for 2 weeks. Each week the alteration in body weights of animals in each group were documented. Following 14 days of treatment, blood was withdrawn from all rats by eye-orbital method and serum was separated from plasma for the biochemical estimation. Then, experimental rats were euthanised by cervical dislocation following overnight starvations. After cervical dislocation, livers were surgically dissected and cleaned carefully by ice cold, phosphate buffer saline (PBS), pH 7.2 (PBS,0.9% w/v) and observed for nodules, foci, lesions and tumors. The liver samples were processed to remove any excess fat, then weighed and divided into small pieces. A portion of the liver tissue was then fixed in buffered formalin for histological examination. In addition, tissue homogenate was prepared by using a slice of liver tissue in neutral phosphate buffer saline of pH 7.

Estimation of Anti-oxidant enzymes

Analysis of the antioxidant enzymes superoxide dismutase (SOD), glutathione reductase (GR), glutathione peroxidase (GPx), and catalase (CAT) was conducted using specific kits as directed by the producer by measuring the absorbance at 440 nm, 412 nm, 340 nm and 520 nm respectively (37).

Lipid peroxidation (LPO) assay

The Sigma kit (MAK085) was used to conduct the LPO assay in accordance with the instructions provided by the manufacturer and the endpoint was assessed at 532 nm wavelength.

Liver marker enzymes

Quantification of hepatic markers i.e., alkaline phosphatase (ALP), aspartate aminotransferase (AST) and alanine aminotransferase (ALT) was carried out to examine the impact of EELS on the restoration of cancerous liver. For this, the liver tissue homogenate was incubated with their respective reagent for min-

utes and measured at 405 nm (ALP) and 570 nm (AST and ALT) with the help of microplate reader following the directions provided by the manufacturer (5).

Estimation of cytokines

Inflammatory biomarkers (TNF-alpha and IL-1β) were estimated by employing their corresponding Enzyme-linked immunosorbent assay (ELISA) kit in accordance with the methodology provided by the manufacturer (5).

Morphological study

For gross morphological study, the excised liver obtained from the sacrificed animals were examined microscopically on the surface as well as on a 3 mm cross-section to check visible hyperplastic nodules of greyish-white colour clearly distinguishable from the surrounding reddish-brown liver. In order to determine the average diameter of each nodule, its nearly spherical shape was measured in two directions that were perpendicular to one another (44).

Histopathological analysis

Following isolation and cleansing, rat liver tissues obtained from each group were fixed using formalin. Afterwards, formalin-fixed samples were treated with increasing strength of ethyl alcohol. Dehydration completion was checked by dipping in xylene and entrenched in paraffin wax to prepare tissue blocks. Tissue blocks were sliced to obtain 5-6 µM sections, deparaffinized, applied with H&E stain and tissue architecture was observed under a microscope.

Cell Proliferation analysis by BrdU assay

Liver tissue sections were deparaffinized, rehydrated, their Ag were retrieved and a thin section (4µm) was dissected out for preparation of slide. It was impedded by incubating with hydrogen peroxide (3%) for 10 minutes. Subsequently, mouse anti-BrdU primary Ab (Bu20a; DAKO, Carpinteria, CA) in 1% BSA was added (dilution 1:500) and incubated throughout the night (4ºC). It was followed by incubation with corresponding secondary Ab (rabbit anti-mouse IgG Ab in a dilution of 1:500; 37ºC, 30 min). At last the tissue section was stained with diaminobenzidine (DAB) and counter stained with haematoxylin before viewing under a microscope (45).

Analysis of PCNA expression

Streptavidin-avidin biotin immunoperoxidase-complex technique was used to detect PCNA expression. After deparaffinization, rehydration and Ag retrieval, the small portion of tissue (5µm) was blocked by incubating half an hour with H_20_2 (1%) in Tris-NaCl (0.1 M, pH 7.6). After incubation with normal goat serum (5%; 37ºC, 1 hr), primary monoclonal mouse anti-PCNA antibody (2µg/ml; Anti PCNA clone #5A10, MBL Co., Ltd. Japan) was added and incubated overnight. Subsequently, the it was incubated with biotinylated secondary antibody anti mouse IgG (Immunopure; 1.5000 dilution; 37°C, 30 min) and streptavidin peroxidase (1:100, 1 hr). Staining was developed with DAB, slides were counterstained with hematoxylin, dehydrated, and mounted. Primary Ab was replaced with PBS to prepare negative control. Prominent reddish-brown colouration depicted PCNA positive cells. In a random high-power field, no. of positive cells with respect to total number of cells was estimated to calculate the PCNA-labelling index using the formula given below (46).

$$\text{PCNA} - \text{labeling index} = \frac{\text{number of PCNA} - \text{positive nuclei}}{\text{total number of nuclei counted}} \times 100$$

Statistical analysis

For statistical analysis one-way analysis of variance (ANOVA) and Bonferroni's multiple comparison test was used keeping sample size uniform. All values were expressed as mean ± standard error mean (SEM) with level of significance $p < 0.05$.

Results and Discussion

Microscopic evaluation

Results of the microscopic evaluation of roots displayed an irregularly circular in outline and shows 4 to 5 tangentially running rows of lignified cork cells; in a few places, the cork tis-

sues are seen exfoliating; underneath the cork wide cortex made up of loosely arranged thin-walled parenchyma cells with few laticiferous cells is present; tannin deposition in some of the cortical cells; starch grains embedded with few cells. The centrally situated vascular bundles cover more than half of the section; the presence of phloem with some sieve tube and companion cells above the xylem; the medullary rays arising from the centre and extending up to the cortex region are multiseriate, barrel-shaped and loaded with some starch grains; xylem with a small pith occupy almost entire portion of the root; is diarch to tetrarch and composed of xylem fibres, vessel and xylem parenchyma (Fig. 1). Petiole is broadly concave on the lower region and irregular on the upper region with two winged projections; outer epidermis is covered by a thin cuticle and is single layered; 4 layers of chlorenchyma cells are seen below; ground tissue is parenchymatous and contains 3 vascular bundles; small vascular bundles are present in the winged region; pericyclic patches are present above the bundles; phloem is present below the xylem elements (Fig. 2). The TS leaf is biconvex with uniseriate upper and lower epidermis covered by distinct cuticle; 3 to 4 layers of chlorenchyma cells are seen below the upper epidermis, followed by 8 to 10 layered thin-walled parenchyma cells forming the ground tissue; a large collateral vascular bundle is present in the center; xylem is composed of protoxylem (oriented towards the upper epidermis) and metaxylem (located towards the lower epidermis) vessels; phloem is present below the xylem; parenchymatous pericycle is seen surrounding the bundle (Fig. 3a). In the lamina, upper and lower uniseriate epidermis is covered by thin cuticle; the dorsiventral mesophyll is distinguished into spongy and palisade parenchyma cells. The palisade parenchyma is 2 to 3 layered and composed of followed by 4 to 5 layers of spongy parenchyma cells; veins are seen traversing through the mesophyll; few oil globules are seen randomly distributed (Fig. 3b). The epidermal peelings of the leaf were observed microscopically, and the quantitative parameters obtained were recorded (Table 1). The leaf was amphistomatic with a uniform distribution of anomocytic stomata on both adaxial and abaxial surfaces (Fig. 4).

Powder microscopy was found to be grey in color with characteristic odour and salty taste and shows fragment of cork, epidermal fragment with anomocytic stomata, parenchyma cells, cells with oil globules, annular, bordered pitted and reticulate vessel, prismatic crystals and starch grains (Fig. 5). Furthermore, the extract was observed to be positive for the presence of alkaloids, triterpenoids, steroids, tannins, glycosides, saponins, carbohydrates, flavonoids, and phenolic compounds (Supplementary Table 1).

Table 1. Quantitative microscopy of *L. sarmentosa* leaf

Parameters	Upper epidermis (/mm^2)	Lower epidermis (/mm^2)
Stomatal number	45-55	60-70
Epidermal number	100-110	120-130
Stomatal index	31-34	33-35
Vein termination	15-20	
Vein islet	8 – 10	
Palisade ratio	18 – 20	

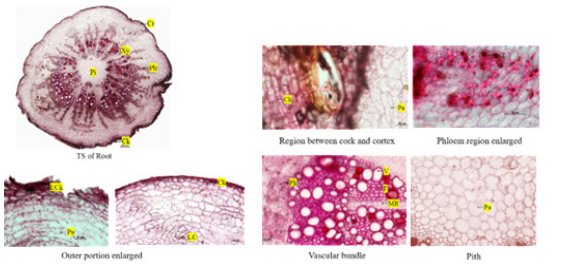

Fig 1. T.S. of *L. sermentosa* Root; where Ck - cork; Ct - cortex; ECk - exfoliating cork; F - fibre; MR - medullary ray; Pa- parenchyma; Ph - phloem; Pi - pith; TC - tannin cell; V - vessel; VB - vascular bundle.

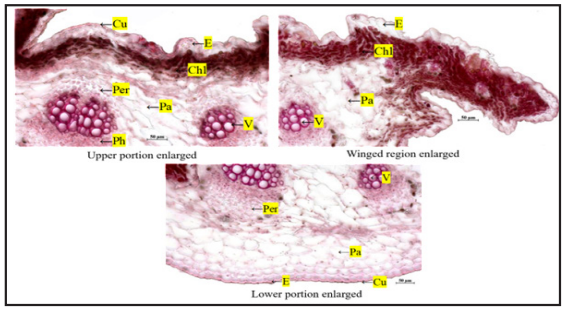

Fig 2. TS of *L. sermentosa* petiole; where Chl - chlorenchyma; Ct - cortex; Cu - cuticle; E - epidermis; Pa- parenchyma; Per - pericycle; Ph - phloem; V - vessel; VB - vascular bundle.

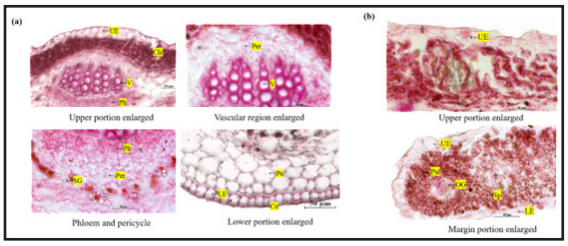

Fig 3. TS of *L. sermentosa* leaf; (a) TS of lamina and (b) TS of midrib; where Chl - chlorenchyma; Col - collenchyma; Cu - cuticle; LE - lower epidermis; Mes - mesophyll; Pa - parenchyma; Ph - phloem; SG - starch grains; UE - upper epidermis; V - vessel; VB - vascular bundle; LE - lower epidermis; OG - oil globule; Pal - palisade parenchyma; SP - spongy parenchyma; UE - upper epidermis; Ve – vein.

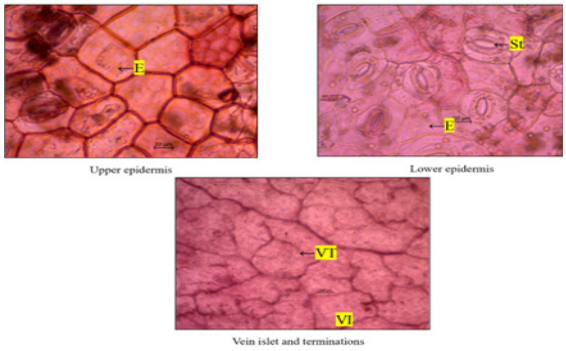

Fig 4. Quantitative microscopy of *L. sarmentosa* leaf by observing upper epidermis and lower epidermis for studying vein islet and vein termination; where E - epidermis; St - stomata; VI - vein islet; VT - vein termination.

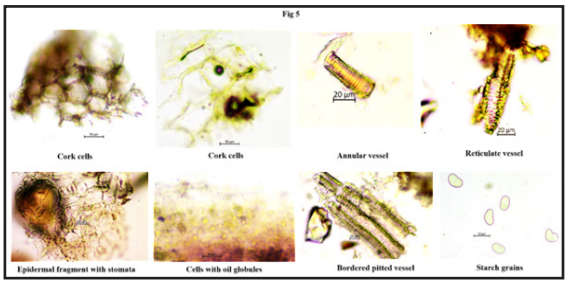

Fig 5. Powder microscopy of *L. sermentosa* root and leaf.

In vitro anti-oxidant efficacy of EELS

The *in vitro* antioxidant activity of the ethanolic extract of *L. sarmentosa* was investigated by three different methods, including hydroxyl radical, DPPH, and nitric oxide scavenging assays, using ascorbic acid as the standard. The IC_{50} values of the extract for hydroxyl radical, DPPH, and nitric oxide scavenging assays were found to be 39.24, 622.85, and 199.84 µg/ml, respectively (Table 2), which is correlated with concentration, i.e., with increasing concentration leading to increased activity. These radicals can induce oxidative damage to DNA, proteins, and lipids, making it important to prevent their formation as a basis for preventing various diseases.

Table 2. IC_{50} value of *In vitro* antioxidant activities of *L.sarmentosa*

Sample	Hydroxyl radical scavenging activity (µg/ml)	DPPH radical scavenging activity (µg/ml)	Nitric oxide radical scavenging activity (µg/ml)
L. sermantosa	39.24	622.85	199.84
Ascorbic acid	21.32	272.39	201.12

In vitro cytotoxicity study

MTT assay was performed to analyze the cytotoxic potential of EELS on HepG2 cell lines. EELS inhibited viability of HepG2 cells in concentration-dependent fashion from 1 µg/ml to 500 µg/ml with an IC_{50} value of 75.25 µg/ml concentration (Table 3). This inhibition of can-

cer cell proliferation was found to be associated with morphological alterations such as shrinkage, cell-distortion as well as rounding of cells relative to the untreated cells as observed under microscope (Data not shown).

Table 3. *In vitro* cytotoxicity study

Concentration (µg/ml)	% cell inhibition *(n=3)*
0	0.00 ± 0.00
1	2.31 ± 0.09
5	5.96 ± 0.18
10	8.91 ± 0.48
50	32.64 ± 1.58
100	67.18 ± 2.31
200	80.20 ± 2.08
500	99.36 ± 4.67

Where, the data are represented as mean ± SEM

EELS altered body weight and liver weight in NDEA induced liver cancer bearing animals

In normal control animals, b.w. increased gradually without any notable abnormal changes during the entire experimental period. After NDEA treatment, a significant decrease ($p < 0.001$) in b.w. was observed in all the animals compared to the normal control group up to 6th week. After treatment with EELS the b.w. of cancer bearing animals was found to be increased significantly. Moreover, group III animals (EELS 100 mg/kg/day) exhibited lowest significant ($p < 0.01$) increase in b.w. while group V animals (EELS 400 mg/kg/day) revealed maximum increase ($p < 0.001$) in b.w. as compared to group II animals (Fig. 6a).

Liver weight was also assessed in all the groups of animals (Fig. 6b). NDEA treated animals showed high significant increase in liver weight ($p < 0.001$) in comparison to normal control animals while liver weight reduced gradually after EELS treatment (groups III, IV, V). In comparison to induced control group, (EELS 100 mg/kg/day) exhibited no significant decrease ($p > 0.05$) in liver weight while higher

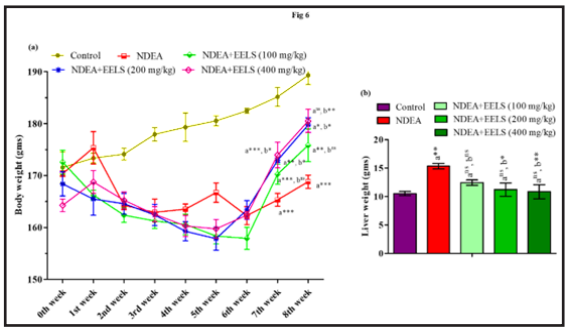

Fig 6. Effect of EELS on alteration in body weight **(a)** and liver weight **(b)** of experimental animals during the study period. Each value is represented as mean ± SEM; n=6. Group I: Control; Group II: NDEA; Group III: NDEA+EELS (100 mg/kg); Group IV: NDEA+EELS (200 mg/kg) and Group V: NDEA+EELS (400 mg/kg). Comparisons: a=group II, III, IV, V with group I; b=group III, IV and V with group II. Significant: $^{ns}p > 0.05$; $^{*}p < 0.05$; $^{**}p < 0.01$; $^{***}p < 0.001$. NDEA: N-Nitrosoethyldiamine, EELS: ethanolic extract of aerial part of *Launaea sarmentosa*.

doses (EELS 200 mg/kg/day and 400 mg/kg/day) caused subsequent normalization of liver weight ($p < 0.05$, $p < 0.01$).

EELS treatment reduced oxidative stress in rats with HCC

When compared to the normal control (Group I), antioxidant enzyme activity (SOD, CAT, GR, and GPx) in the NDEA-treated group (Group II) was significantly reduced. EELS-treated groups (III, IV, V) showed a sig-

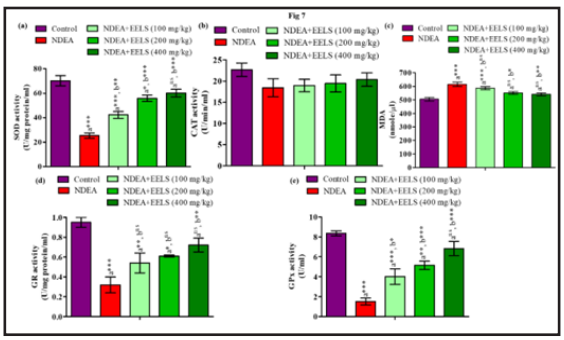

nificant increase ($p < 0.05$) in enzyme activity (Fig. 7a, c, d, e), except for CAT (statistically

non-significant) [Fig. 7b] compared to the induced control.

Fig 7. Analysis of enzymatic and non-enzymatic antioxidants and lipid peroxidation levels of rats treated with EELS following NDEA induced HCC i.e., **(a)** Superoxide dismutase (SOD), **(b)** Catalase (CAT), **(c)** Malonaldehyde (MDA), **(d)** Glutathione reductase (GR) **(e)** Glutathione peroxidase (GPx). Each value is represented as mean ± SEM; n=6. Group I: Control; Group II: NDEA; Group III: NDEA+EELS (100 mg/kg); Group IV: NDEA+EELS (200 mg/kg) and Group V: NDEA+EELS (400 mg/kg). Comparisons: a=group II, III, IV, V with group I; b=group III, IV and V with group II. Significant: $^{ns}p > 0.05$; *p < 0.05; **p < 0.01; ***p < 0.001. NDEA: N-Nitrosoethyldiamine, EELS: ethanolic extract of aerial part of *Launaea sarmentosa*.

EELS restored altered liver enzymes

In the NDEA-treated groups (II, III, IV, and V), liver enzyme activity (ALP, ALT, AST) increased compared to the normal untreated

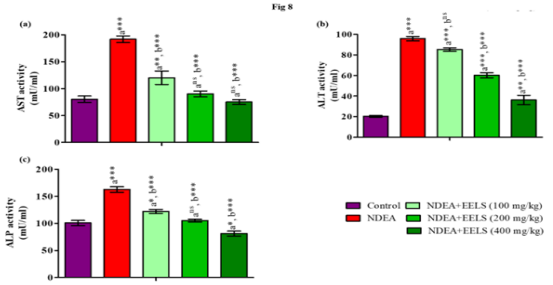

control (Group I). The EELS-treated groups (III, IV, and V) showed a statistically significant decrease ($p < 0.05$) in enzyme activity compared to the NDEA-induced control (Fig. 8a-c).

Fig 8. Analysis of liver marker enzymes of rats treated with EELS following NDEA induced HCC i.e., **(a)** Aspartate aminotransferase **(**AST), **(b)** Alanine aminotransferase (ALT) and **(c)** Alkaline phosphatase (ALP). Each value is represented as mean ± SEM; n=6. Group I: Control; Group II: NDEA; Group III: NDEA+EELS (100 mg/kg); Group IV: NDEA+EELS (200 mg/kg) and Group V: NDEA+EELS (400 mg/kg). Comparisons: a=group II, III, IV, V with group I; b=group III, IV and V with group II. Significant: $^{ns}p > 0.05$; *p < 0.05; **p < 0.01; ***p < 0.001. NDEA: N-Nitrosoethyldiamine, EELS: ethanolic extract of aerial part of *Launaea sarmentosa*.

EELS treatment inhibits pro-inflammatory cytokines

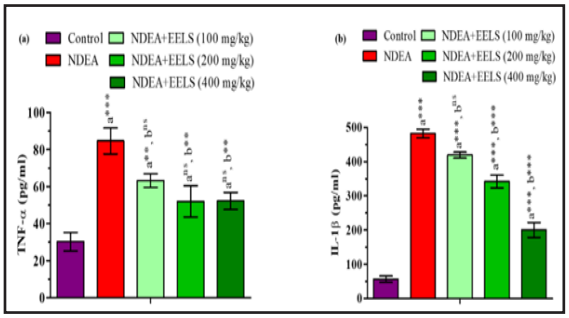

A significant increase ($p < 0.001$) in the inflammatory markers (TNF-α and IL-1β) was observed in NDEA-induced hepatotoxic rats compared to the control group (Fig. 9). However, treatment with EELS at a higher dose (400 mg/kg b.w.) significantly decreased these inflammatory marker levels ($p < 0.001$).

Fig 9. Analysis of inflammatory cytokines in serum samples of rats treated with EELS following NDEA induced HCC i.e., **(a)** Tumour Necrosis Factor-α **(**TNF-α) and **(b)** Interleukin-1β (IL-1β). Each value is represented as mean ± SEM; n=6. Group I: Control; Group II: NDEA; Group III: NDEA+EELS (100 mg/kg); Group IV: NDEA+EELS (200 mg/kg) and Group V: NDEA+EELS (400 mg/kg). Comparisons: a=group II, III, IV, V with group I; b=group III, IV and V with group II. Significant: $^{ns}p > 0.05$; *p < 0.05; **p < 0.01; ***p < 0.001. NDEA: N-Nitrosoethyldiamine, EELS: ethanolic extract of aerial part of *Launaea sarmentosa*.

Treatment with EELS restores normal liver architecture

The appearance of hepatic hyperplastic nodules as judged by their percentage of inci-

dence and number of nodules. One single dose of NDEA resulted in 92% incidence of hyperplastic nodules, from which nearly 7.5% nodules have a size of more than 3 mm. However, administration of EELS for 14 consecutive days repressed these nodules, having maximum inhibition (75%) at the dose of 400 mg/kg (Table 4).

Table 4. Effect of EELS in development of nodular hyperplasia in rats with HCC

Group	% incidence of nodules	% inhibition of nodules	% of nodules relative to size		
			<1 mm	1-3 mm	>3 mm
NDEA	92%	-	16.2	76.3	7.5
NDEA+EELS (100 mg/kg)	90%	30%	55.6	43.2	1.2
NDEA+EELS (200 mg/kg)	83%	59%	64	36	0
NDEA+EELS (400 mg/kg)	86%	75%	75.9	24.2	0

Where, the data are represented as n=6.

EELS restored altered liver histology

As depicted in Fig. 10, control rats displayed normal liver parenchyma with granular cytoplasm. Small uniform nuclei can be seen radially arranged the central vein [Fig. 10a(i)]. Induction of HCC phenotypically altered the architecture of hepatocytes. Multinucleated, hyperchromatic, oval, irregular hepatocytes having consistent focal lesion and nodules were observed. Portal veins were encircled by prominent hyper basophilic mass i.e., clearly distinguishable from surrounding non-nodular parenchyma. Nucleus were found to be large with centrally located nucleoli and surrounded by highly vacuolated cytoplasm containing masses of eosinophilic substances [Fig. 10a(ii)]. Treatment with EELS (100 mg/kg) reduces the no. of multi-nucleated hepatic cells, reduced the nucleus size and improved vacuolation and compactness of hepatocytes, however, still some heterogeneity can be noticed. Basophilic cells can be perceived to be scattered in the cytoplasm without being aggregated around the portal vein [Fig. 10a(iii)]. These alterations can be ameliorated and normal tissue architecture was restored on administration of higher doses of EELS [Fig. 10a(iv and v)].

Effect of EELS on BrdU expression

A significant immunolocalization of BrdU-immuno positive hepatocytes was observed in NDEA-induced group (BrdU-Li: 25.3±0.27) as compare to normal animals (BrdU-Li: 13.2±0.32) depicting strong immunoreactivity. Nevertheless, treatment with EELS showed a moderate to low BrdU labelling with minimal focal areas and scattered BrdU positive cells (Fig. 10b and Table 5).

Table 5. Cell proliferative marker study

Group	BrdU-labelling index (BrdU-Li)	PCNA-labelling index (PCNA-Li)
Control	13.2±0.32	12.52±0.63
NDEA	25.3±0.27	28.39±0.25
NDEA+EELS (100 mg/kg)	21.6±0.16	22.05±0.39
NDEA+EELS (200 mg/kg)	17.5±0.28	21.10±0.42
NDEA+EELS (400 mg/kg)	16.2±0.21	19.39±0.68

Where, the data are represented as mean ± SEM values (n=6) and significance of difference is indicated as ***p < 0.001, **p < 0.01, *p < 0.05 and nsp > 0.05. Effect of EELS on PCNA expression

Current Trends in Biotechnology and Pharmacy
Vol. 19(3) 2462-2479, July 2025, ISSN 0973-8916 (Print), 2230-7303 (Online)
DOI: 10.5530/ctbp.2025.3.30

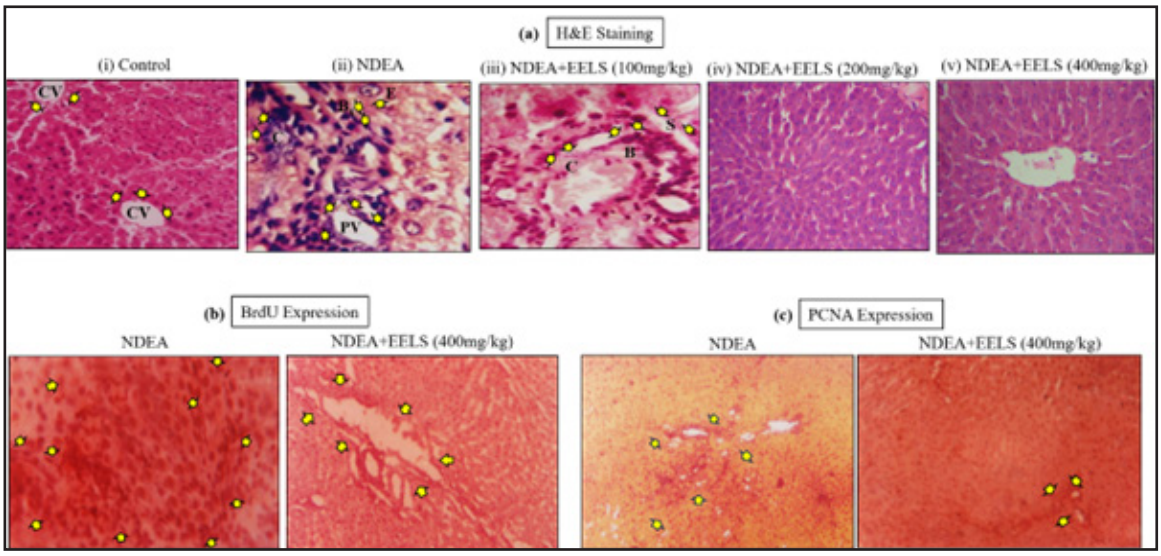

Fig 10. **(a)** Alteration in liver histology observed after Haematoxylin and eosin (H&E) staining, **(b)** Microscopical images of liver tissue section showcasing BrdU expression profile following immunostaining and **(c)** Microscopical images showcasing PCNA expression profile following immunostaining. NDEA: N-Nitrosoethyldiamine, EELS: ethanolic extract of aerial part of *Launaea sarmentosa*, BrdU: Bromodeoxyuridine or 5-bromo-2'-deoxyuridine, PCNA: Proliferating cell nuclear antigen.

Since PCNA plays an important role in DNA replication, we have the in situ estimated localization of PCNA expression in rat liver depicted in Fig. 10c. Intense immunostaining of PCNA along with clusters of focal expression inside precancerous lesion was observed in NDEA-induced group (PCNA-Li: 28.39±0.25), suggesting higher rate of cell proliferation upon cancer induction. This proliferative marker reduced in a dose-dependent manner following treatment with EELS (Fig. 10c and Table 5).

Discussion

Pathologic and metabolic changes induced by disproportionate antioxidant status result in damaged cellular cohesiveness, fostering the development of tumor (47). Preliminary phytochemical investigation found antioxidant-potent phytoconstituents (phenols, flavonoids, alkaloids, glycosides, saponins, triterpenes, carbohydrates, steroids, tannins) in L.sermentosa. The preliminary phytochemical investigation found antioxidant-potent phytoconstituents (phenols, flavonoids, alkaloids, glycosides, saponins, triterpenes, carbohydrates, steroids, and tannins) in L.sermentosa. Reactive oxygen species (ROS) can cause oxidization of protein, DNA and lipid and hence, prevention of ROS is essential to reducing the risk of numerous diseases, including cancer (48). *In vitro* antioxidant assay exhibited a notable scavenging action against H_2O_2, DPPH, and NO radicals. A prominent surge in DPPH, H_2O_2 and NO can occur due to stress. DPPH is a lipophilic radical which participates in lipid autoxidation chain reactions. It is a very stable radical that can consume hydrogen or electron to generate a diamagnetic molecule. Antioxidants lower DPPH absorbance at 517 nm, indicating its reducing capacity (49). A positive DPPH test reveals L.sermentosa scavenges free radicals. NO, a pro-inflammatory mediator generated when sodium nitroprusside breaks down at physiological pH, contributes to inflammation (37). Oxidative stress is also caused by oxygen-derived free radicals like hydrogen peroxide (H_2O_2). L.sermentosa showed radical scavenging activity comparable to ascorbic acid.

Subsequently, the effectiveness of EELS was estimated in an *in vivo* rat model of N-nitroso diethylamine (NDEA)-induced HCC. NDEA is a potent carcinogen that develops HCC by hindering DNA and RNA-repairing pathways, thereby triggering oxidative stress by initiating free radicals production (50). CytP450 (CYP2E1) metabolizes NDEA into 6-ethyldeoxythymidine and 4-ethyl-deoxyguanosine within liver. CCl_4 also causes endoplasmic reticulum to produce trichloromethyl free radicals that interact with cellular lipid and protein to form peroxyl radicals. These radicals damage cell membrane lipids and proteins, increasing carcinogenic complexity (51,52). Since, NDEA is a widely available environmental pollutant found in chemical used in agriculture, industry, packaged drinks, tobacco smoke etc. precipitating liver diseases (53), its employment as a typical hepatocellular carcinoma screening model for antioxidant-rich hepatoprotective drugs is favourable.

The current study revealed a noteworthy decrease in b.w. in the NDEA treated group compared to the control animals, which may be attributed to stress. During the course of the experiment, it was seen that the dietary intake of rats decreased, resulting in a sudden fall in b.w. due to defective metabolism and liver toxicity (54). However, the administration of EELS resulted in a significant improvement of this condition depending on the drug concentration. Spontaneous cell replication takes place in the hepatic lobules during the regular developmental process and regeneration, in case of minimal tissue loss or after the end of the injury phase. A deficit of more than 20-30% limits the proliferation (55). The carcinogenic animals exhibited a substantial rise in liver weight, as compared to that of the normal animals, due to accelerated cell replication and an augmented tumour burden, which get ameliorated upon administration of EELS.

Elevated levels of ROS due to oxidative stress with reduced antioxidants trigger tissue damage (56). Antioxidant enzymes are popular for their capacity to prevent carcinogen-induced ROS generation in rats. The anti-oxidant enzyme SOD translates O_2- into O_2 and H_2O_2, thereby fortifying from its harmful effects. Further, CAT converts H_2O_2 into H_2O, completely neutralising free radicals. The enzyme GPx is a protein containing selenium, which is located in the mitochondrial matrix and cytoplasm of the cell (57). Together with glutathione, it shields the cell from oxidative damage (58). Another enzyme GR reduces oxidized glutathione (GSSG) into GSH. The NDEA-treated group exhibited a significant decrease in anti-oxidant proteins. However, EELS ingestion ameliorates these effects, suggesting the oxidative stress-reducing capability of EELS. MDA is the final product of Lipid peroxidation (LPO) of polyunsaturated fatty acids, which can initiate the formation of cross-links within proteins, lipids, and nucleic acids. Thus, the amount of LPO was elevated in carcinogenesis, which aligns with our research findings (59). However, normalcy was restored upon ingestion of EELS.

Carcinogens like NDEA and CCl_4 trigger impairment of hepatic cells leading to the release of liver marker enzymes into the bloodstream (60,61) and treatment with hepatoprotective agent restored their levels to normalcy (62). We found that EELS dose-dependently restored the level of AST, ALT and ALP in rats compared to carcinogen-induced animals. This proves that EELS regenerates parenchymal cells and reduces enzymatic linkage by maintaining membrane integrity. Cytokines are a kind of immune system pleiotropic hormones that contribute towards neoplastic induction, maintenance and advancement (63). In general, neoplastic cells and tumor-associated macrophages (TAM) promote tumor development by inducing the release of inflammatory markers (TNF-α, IL-1β, and angiogenic and lymphangiogenic growth factors) (64,65). Our study recorded elevated serum levels of these proinflammatory cytokines in the NDEA treatment groups, while EELS therapy effectively attenuated their levels.

NDEA treatment disrupts the liver's normal histological architecture (hexagonal lobular structure with radially arranged hepatocytes, the central vein in the middle, and the peripheral portal triad) due to a cascade of events initiated by oxidative stress, leading to membrane damage, inflammatory cell infiltration, cellular atypia, and eventually transformation into HCC (65). However, partial to complete restoration of the liver's histological features was observed following treatment with EELS. This reversal of toxic effects is likely due to the reduction or complete inhibition of NDEA-induced oxidative stress and improved antioxidant status. PCNA is an auxiliary protein of DNA polymerase δ and its expression is increased in proliferating cells. Combined with histopathological characteristics, a high frequency of PCNA overexpression is a reliable marker for evaluating malignant grades or stages of tumor differentiation and the assessment of tumor progression. In our study, localized expression of PCNA in areas of high proliferative activity was observed which might be an early event in the pathogenesis of hepatic neoplasia. EELS-mediated suppression of PCNA, reflects anti-proliferative activity of EELS. Moreover, a profound decline in the level of BrdU positive cell supports this claim.

Conclusion

Our result clearly demonstrated significant chemotherapeutic potential of EELS against HCC induced by NDEA+phenobarbital+CCl_4 in Wister rats. A marked improvement in morphological and histological features along with amelioration of antioxidant, anti-inflammatory and liver biomarkers were observed following EELS treatment. This effect may attribute to the phytochemical richness of the plant which are known to exert antioxidant and antiproliferative properties. These discoveries could certify the anticancer activity of L.sementosa and postulate it as a functional food to treat liver carcinogenesis.

Acknowledgement

All the authors extend their sincere acknowledgement to the Centurion University of Technology and Management, Odisha for providing the necessary laboratory resources.

Conflict of interest

The authors declare that they have no conflicts of interest.

References

1. Donne, R. and Lujambio, A., 2023. The liver cancer immune microenvironment: Therapeutic implications for hepatocellular carcinoma. Hepatology, 77(5), pp.1773-1796. https://doi.org/10.1002/hep.32740
2. Choo, S.P., Tan, W.L., Goh, B.K., Tai, W.M. and Zhu, A.X., 2016. Comparison of hepatocellular carcinoma in E astern versus W estern populations. *Cancer*, *122*(22), pp.3430-3446. https://doi.org/10.1002/cncr.30237
3. Siegel, R.L., Miller, K.D., Wagle, N.S. and Jemal, A., 2023. Cancer statistics, 2023. *CA: a cancer journal for clinicians*, *73*(1), pp.17-48. https://doi.org/10.3322/caac.21763
4. https://www.who.int/news-room/fact-sheets/detail/cancer#:~:text=liver%20(830%20000%20deaths)%3B, b. d. Accessed on 01.12.2023.
5. Khan, F., Khan, T.J., Kalamegam, G., Pushparaj, P.N., Chaudhary, A., Abuzenadah, A., Kumosani, T., Barbour, E. and Al-Qahtani, M., 2017. Anti-cancer effects of Ajwa dates (Phoenix dactylifera L.) in diethylnitrosamine induced hepatocellular carcinoma in Wistar rats. *BMC complementary and alternative medicine*, *17*, pp.1-10. https://doi.org/10.1186/s12906-017-1926-6
6. Atanasov, A.G., Waltenberger, B., Pferschy-Wenzig, E.M., Linder, T., Wawrosch, C., Uhrin, P., Temml, V., Wang, L., Schwaiger, S., Heiss, E.H. and Rollinger, J.M., 2015. Discovery and resupply of

pharmacologically active plant-derived natural products: A review. *Biotechnology advances*, *33*(8), pp.1582-1614. https://doi.org/10.1016/j.biotechadv.2015.08.001

7. Mohan, S., Maurya, A. and Singh, R.M., 2025. Phytomolecules from herbs: Possible effective way for the treatment of liver cancer. Current Topics in Medicinal Chemistry. https://doi.org/10.2174/0115680266321814250228070642

8. Parfait, B.T.S. and Lawrence, M.T.J., 2023. Pharmacognosy, phytotherapy and modern medicine. Int. J. Infect. Dis. Epidemol, 23(4), p.1. https://doi.org/10.51626/ijide.2023.04.00041

9. Pitakpawasutthi, Y., Palanuvej, C. and Ruangrungsi, N., 2018. Microscopic leaf constant numbers of Chromolaena odorata in Thailand. *Pharmacognosy Journal*, *10*(6s). https://doi.org/10.5530/pj.2018.6s.18

10. Ullah, H.A., Zaman, S., Juhara, F., Akter, L., Tareq, S.M., Masum, E.H. and Bhattacharjee, R., 2014. Evaluation of antinociceptive, in-vivo & in-vitro anti-inflammatory activity of ethanolic extract of Curcuma zedoaria rhizome. *BMC complementary and alternative medicine*, *14*, pp.1-12. https://doi.org/10.1186/1472-6882-14-346

11. Belwal, C., Goyal, P.K., Balte, A., Kolhe, S., Chauhan, K., Rawat, A.S. and Vardhan, A., 2014. Isolation, identification, and characterization of an unknown impurity in lovastatin EP. *Scientia Pharmaceutica*, *82*(1), p.43. https://doi.org/10.3797/scipharm.1305-04

12. Alamgir, A.N.M., 2017. *Therapeutic use of medicinal plants and their extracts: volume 1*. Springer International Publishing AG. https://doi.org/10.1007/978-3-319-92387-1

13. Jones, W.P., Chin, Y.W. and Kinghorn, A.D., 2006. The role of pharmacognosy in modern medicine and pharmacy. *Current drug targets*, *7*(3), pp.247-264. https://doi.org/10.2174/138945006776054915

14. Lalthanpuii, P.B. and Lalchhandama, K., 2020. Phytochemical analysis and in vitro anthelmintic activity of Imperata cylindrica underground parts. *BMC Complementary Medicine and Therapies*, *20*, pp.1-9. https://doi.org/10.1186/s12906-020-03125-w

15. Ukwubile, C.A., Ahmed, A., Katsayal, U.A., Ya'u, J. and Mejida, S., 2019. GC–MS analysis of bioactive compounds from Melastomastrum capitatum (Vahl) Fern. leaf methanol extract: An anticancer plant. *Scientific African*, *3*, p.e00059. https://doi.org/10.1016/j.sciaf.2019.e00059

16. Zhang, F., Xu, Y., Pan, Y., Sun, S., Chen, A., Li, P., Bao, C., Wang, J., Tang, H. and Han, Y., 2019. Effects of Angiotensin-(1-7) and Angiotensin II on Acetylcholine-Induced Vascular Relaxation in Spontaneously Hypertensive Rats. *Oxidative medicine and cellular longevity*, *2019*(1), p.6512485. https://doi.org/10.1155/2019/6512485

17. Beena, K.R., Ananda, K. and Sridhar, K.R., 2000. Fungal endophytes of three sand dune plant species of west coast of India. *SYDOWIA-HORN-*, *52*(1), pp.1-9.

18. JU, S.K., MJ, K.C., Semotiuk, A.J. and Krishna, V., 2019. Indigenous knowledge on medicinal plants used by ethnic communities of South India. *Ethnobotany Research and Applications*, *18*, pp.1-112.

19. Hiremath, B.S. and Chennaveeraiah, M.S., 1988. Cytological studies in Launaea pinnatifida Cass. *Proceedings: Plant Sciences*, *98*, pp.395-398. https://doi.org/10.1007/BF03053440

20. Tetali, P., Waghchaure, C., Daswani, P.G., Antia, N.H. and Birdi, T.J., 2009. Ethnobotanical survey of antidiarrhoeal plants of Parinche valley, Pune district, Maharashtra, India. *Journal of ethnopharmacology*, *123*(2), pp.229-236. https://doi.

org/10.1016/j.jep.2009.03.013

21. Chandak, K.K. and Wasule, D.D., 2021. Wound healing potential of Launaea pinnati ida Cass leaf juice in rats. https://doi.org/10.26452/ijrps.v12i3.4830

22. Shaikh SS (2022). Formulation of herbal ointment for assessment of wound healing activity from leaves. Int J Pharm Chem Anal. 9:79-86. https://doi.org/https://doi.org/10.18231/j.ijpca.2022.013

23. Moghal, M.M.R., Millat, M.S., Hussain, M.S. and Islam, M.R., 2016. Thrombolytic and membrane stabilizing activities of Launaea sarmentosa. *Int J Pharmacog*, *3*(8), pp.354-358. https://doi.org/10.13040/IJPSR.0975-8232.IJP.3(8).354-58

24. Kader, M.A., Hasan, M.R., Parvez, G.M. and Parvin, S., 2022. Phytochemical Screening and Antimicrobial Evaluation of Various Fractionates of Ethanolic Extract of Launaea sarmentosa (Willd.), in the Search of Possible Candidates to Multidrug Resistant Microbes. *Journal of Pharmaceutical Sciences and Research*, *14*(7), pp.811-817.

25. Millat, M.S., Islam, S., Hussain, M.S., Moghal, M.M.R. and Islam, T., 2017. Antibacterial profiling of Launaea sarmentosa (Willd.) and Bruguiera cylindrica (L.): Two distinct ethno medicinal plants of Bangladesh. *Eur Exp Biol*, *7*(6). https://doi.org/10.21767/2248-9215.100006

26. Raju, G.S., RahmanMoghal, M.M., Hossain, M.S., Hassan, M.M., Billah, M.M., Ahamed, S.K. and Rana, S.M., 2014. Assessment of pharmacological activities of two medicinal plant of Bangladesh: Launaea sarmentosa and Aegialitis rotundifolia roxb in the management of pain, pyrexia and inflammation. *Biological research*, *47*, pp.1-11. https://doi.org/10.1186/0717-6287-47-55

27. Nguyen, T.Q., Binh, T.D., Kusunoki, R., Pham, T.L., Nguyen, Y.D., Nguyen, T.T., Kanaori, K. and Kamei, K., 2020. Effects of Launaea sarmentosa extract on lipopolysaccharide-induced inflammation via suppression of NF-κB/MAPK signaling and Nrf2 activation. *Nutrients*, *12*(9), p.2586. https://doi.org/10.3390/nu12092586

28. Them, L.T., Tuong Nguyen Dung, P., Thi Nhat Trinh, P., Tong Hung, Q., Tuong Vi, L.N., Trong Tuan, N., Duc Lam, T., Thuy Nguyen, V. and Dung, L.T., 2019, June. Saponin, Polyphenol, flavonoid content and α-glucosidase Inhibitory activity, antioxidant potential of launaea sarmentosa leaves grown in ben tre province, Vietnam. In *IOP Conference Series: Materials Science and Engineering* (Vol. 542, No. 1, p. 012036). IOP Publishing. https://doi.org/10.1088/1757-899X/542/1/012036

29. Makwana, H.T. and Pandya, D.J., 2019. Launaea pinnatifida cass. A species of the controversial drug gojihva: Comprehensive review. *Int. J. Pharmacogn. Phytochem. Res*, *11*, pp.240-243.

30. Cheriti, A., Belboukhari, M., Belboukhari, N. and Djeradi, H., 2012. Phytochemical and biological studies on Launaea Cass. genus (Asteraceae) from Algerian Sahara. *Phytochemistry*, *11*, pp.67-80.

31. Hanh, L.H., Dung, P.D., Huy, L.D., Duong, N.T.T., Wacharasindhu, S., Phung, N.K.P. and Chi, H.B.L., 2020. Chemical constituents of Launaea sarmentosa roots. *Vietnam Journal of Chemistry*, *58*(5), pp.637-642. https://doi.org/10.1002/vjch.202000057

32. Mashlawi, A.M., Alanazi, N.A.H., Mohamed, G., Alfattah, M.A., Mohamed, D.A., Fayad, E. and Salama, S.A., 2024. Exploring the Phytochemical Composition of Methanolic Extract from Launaea nudicaulis: Investigating its Antioxidant, Anticancer, and Anti-Dengue Activities against Aedes aegypti. *Journal of Bioscience and*

Applied Research, *10*(1), pp.30-41. https://doi.org/10.21608/JBAAR.2024.343721

33. Fukumura, H., Sato, M., Kezuka, K., Sato, I., Feng, X., Okumura, S., Fujita, T., Yokoyama, U., Eguchi, H., Ishikawa, Y. and Saito, T., 2012. Effect of ascorbic acid on reactive oxygen species production in chemotherapy and hyperthermia in prostate cancer cells. *The Journal of Physiological Sciences*, *62*, pp.251-257. https://doi.org/10.1007/s12576-012-0204-0

34. Nooreen, Z., Singh, S., Singh, D.K., Tandon, S., Ahmad, A. and Luqman, S., 2017. Characterization and evaluation of bioactive polyphenolic constituents from Zanthoxylum armatum DC., a traditionally used plant. *Biomedicine & Pharmacotherapy*, *89*, pp.366-375. https://doi.org/10.1016/j.biopha.2017.02.040

35. Gülçin, İ., 2005. The antioxidant and radical scavenging activities of black pepper (Piper nigrum) seeds. *International journal of food sciences and nutrition*, *56*(7), pp.491-499. https://doi.org/10.1080/09637480500450248

36. Kota, P., Sahu, P.K., Palla, M.S., Panda, J., Damarasingu, P. and Ranajit, S.K., 2023. Pharmacognostic and pharmacological perspectives of Leea macrophyla roxb. *Advances in Traditional Medicine*, *23*(4), pp.1123-1136. https://doi.org/10.1007/s13596-022-00656-0

37. Sahu, R., Kar, R.K., Sunita, P., Bose, P., Kumari, P., Bharti, S., Srivastava, S. and Pattanayak, S.P., 2021. LC-MS characterized methanolic extract of zanthoxylum armatum possess anti-breast cancer activity through Nrf2-Keap1 pathway: An in-silico, in-vitro and in-vivo evaluation. *Journal of Ethnopharmacology*, *269*, p.113758. https://doi.org/10.1016/j.jep.2020.113758

38. Sreejayan, X.X. and Rao, M.N.A., 1997. Nitric oxide scavenging by curcuminoids. *Journal of pharmacy and Pharmacology*, *49*(1), pp.105-107. https://doi.org/10.1111/j.2042-7158.1997.tb06761.x

39. Blois, M.S., 1958. Antioxidant determinations by the use of a stable free radical. *Nature*, *181*(4617), pp.1199-1200. https://doi.org/10.1038/1811199a0

40. Shrivastava, A.K., Sahu, P.K., Cecchi, T., Shrestha, L., Shah, S.K., Gupta, A., Palikhey, A., Joshi, B., Gupta, P.P., Upadhyaya, J. and Paudel, M., 2023. An emerging natural antioxidant therapy for COVID-19 infection patients: Current and future directions. *Food Frontiers*, *4*(3), pp.1179-1205. https://doi.org/10.1002/fft2.207

41. Pound, A.W., Lawson, T.A. and Horn, L., 1973. Increased carcinogenic action of dimethylnitrosamine after prior administration of carbon tetrachloride. *British journal of cancer*, *27*(6), pp.451-459. https://doi.org/10.1038/bjc.1973.57

42. Yadav, A.S. and Bhatnagar, D., 2007. Chemo-preventive effect of Star anise in N-nitrosodiethylamine initiated and phenobarbital promoted hepato-carcinogenesis. *Chemico-biological interactions*, *169*(3), pp.207-214. https://doi.org/10.1016/j.cbi.2007.06.032

43. Pattanayak, S.P., Bose, P., Sunita, P., Siddique, M.U.M. and Lapenna, A., 2018. Bergapten inhibits liver carcinogenesis by modulating LXR/PI3K/Akt and IDOL/LDLR pathways. *Biomedicine & Pharmacotherapy*, *108*, pp.297-308. https://doi.org/10.1016/j.biopha.2018.08.145

44. Moreno, F.S., Rizzi, M.B.S.L., Dagli, M.L.Z. and Penteado, M.D.V.C., 1991. Inhibitory effects of β-carotene on preneoplastic lesions induced in Wistar rats by the resistant hepatocyte model. *Carcinogenesis*, *12*(10), pp.1817-1822. https://doi.org/10.1093/carcin/12.10.1817

45. Hao, W.C., Zhong, Q.L., Pang, W.Q., Dian,

M.J., Li, J., Han, L.X., Zhao, W.T., Zhang, X.L., Xiao, S.J., Xiao, D. and Lin, X.L., 2020. MST4 inhibits human hepatocellular carcinoma cell proliferation and induces cell cycle arrest via suppression of PI3K/AKT pathway. *Journal of Cancer*, *11*(17), p.5106. https://doi.org/10.7150/jca.45822

46. Kumar, A., Sunita, P., Jha, S. and Pattanayak, S.P., 2018. 7, 8-Dihydroxycoumarin exerts antitumor potential on DMBA-induced mammary carcinogenesis by inhibiting ERα, PR, EGFR, and IGF1R: involvement of MAPK1/2-JNK1/2-Akt pathway. *Journal of physiology and biochemistry*, *74*, pp.223-234. https://doi.org/10.1007/s13105-018-0608-2

47. Batcioglu, K., Uyumlu, A.B., Satilmis, B., Yildirim, B., Yucel, N., Demirtas, H., Onkal, R., Guzel, R.M. and Djamgoz, M.B., 2012. Oxidative Stress in the in vivo DMBA Rat Model of Breast Cancer: Suppression by a Voltage-gated Sodium Channel Inhibitor (RS 100642). *Basic & clinical pharmacology & toxicology*, *111*(2), pp.137-141. https://doi.org/10.1111/j.1742-7843.2012.00880.x

48. Spencer, J.P., Jenner, A., Aruoma, O.I., Evans, P.J., Kaur, H., Dexter, D.T., Jenner, P., Lees, A.J., Marsden, D.C. and Halliwell, B., 1994. Intense oxidative DNA damage promoted by l-DOPA and its metabolites implications for neurodegenerative disease. *FEBS letters*, *353*(3), pp.246-250. https://doi.org/10.1016/0014-5793(94)01056-0

49. Pattanayak, S.P., Mazumder, P.M. and Sunita, P., 2011. Total phenolic content, flavonoid content and in vitro antioxidant activities of Dendrophthoe falcata (Lf) Ettingsh. *Int J PharmTech Res*, *3*, pp.1392-406.

50. Choo, S.P., Tan, W.L., Goh, B.K., Tai, W.M. and Zhu, A.X., 2016. Comparison of hepatocellular carcinoma in E astern versus W estern populations. *Cancer*, *122*(22), pp.3430-3446. https://doi.org/10.1002/cncr.30237

51. Rao, G.M.M., Rao, C.V., Pushpangadan, P. and Shirwaikar, A., 2006. Hepatoprotective effects of rubiadin, a major constituent of Rubia cordifolia Linn. *Journal of ethnopharmacology*, *103*(3), pp.484-490. https://doi.org/10.1016/j.jep.2005.08.073

52. Xu, M., Zhao, Q., Shao, D., Liu, H., Qi, J. and Qin, C., 2017. Chenodeoxycholic Acid Derivative HS-1200 Inhibits Hepatocarcinogenesis and Improves Liver Function in Diethylnitrosamine-Exposed Rats by Downregulating MTH1. *BioMed Research International*, *2017*(1), p.1465912. https://doi.org/10.1155/2017/1465912

53. Raghunandhakumar, S., Paramasivam, A., Senthilraja, S., Naveenkumar, C., Asokkumar, S., Binuclara, J., Jagan, S., Anandakumar, P. and Devaki, T., 2013. Thymoquinone inhibits cell proliferation through regulation of G1/S phase cell cycle transition in N-nitrosodiethylamine-induced experimental rat hepatocellular carcinoma. *Toxicology letters*, *223*(1), pp.60-72. https://doi.org/10.1016/j.toxlet.2013.08.018

54. Lee, S.J. and Boyer, T.D., 1993. The effect of hepatic regeneration on the expression of the glutathione S-transferases. *Biochemical Journal*, *293*(1), pp.137-142. https://doi.org/10.1042/bj2930137

55. Kato, H. and Shimazu, T., 1983. Effect of autonomic denervation on DNA synthesis during liver regeneration after partial hepatectomy. *European journal of biochemistry*, *134*(3).

56. Huang, Y.L., Sheu, J.Y. and Lin, T.H., 1999. Association between oxidative stress and changes of trace elements in patients with breast cancer. *Clinical biochemistry*, *32*(2), pp.131-136. https://doi.org/10.1016/S0009-9120(98)00096-4

57. Xiong, Y., Wang, K., Zhou, H., Peng, L., You, W. and Fu, Z., 2018. Profiles of immune infiltration in colorectal cancer and their clinical significant: A gene expression-based study. *Cancer medicine*, *7*(9), pp.4496-4508. https://doi.org/10.1002/cam4.1745

58. Cerutti, P., Ghosh, R., Oya, Y. and Amstad, P., 1994. The role of the cellular antioxidant defense in oxidant carcinogenesis. *Environmental health perspectives*, *102*(suppl 10), pp.123-129. https://doi.org/10.1289/ehp.94102s10123

59. Pattanayak, S.P. and Mazumder, P.M., 2011. Therapeutic potential of Dendrophthoe falcata (Lf) Ettingsh on 7, 12-dimethylbenz (a) anthracene-induced mammary tumorigenesis in female rats: effect on antioxidant system, lipid peroxidation, and hepatic marker enzymes. *Comparative clinical pathology*, *20*, pp.381-392. https://doi.org/10.1007/s00580-010-1008-3

60. Azri, S., Mata, H.P., Reid, L.L., Gandolfi, A.J. and Brendel, K., 1992. Further examination of the selective toxicity of CCl4 in rat liver slices. *Toxicology and applied pharmacology*, *112*(1), pp.81-86. https://doi.org/10.1016/0041-008X(92)90282-W

61. Sivaramakrishnan, V., Shilpa, P.N.M., Kumar, V.R.P. and Devaraj, S.N., 2008. Attenuation of N-nitrosodiethylamine-induced hepatocellular carcinogenesis by a novel flavonol—Morin. *Chemico-biological interactions*, *171*(1), pp.79-88. https://doi.org/10.1016/j.cbi.2007.09.003

62. Abdelaziz, D.H. and Ali, S.A., 2014. The protective effect of Phoenix dactylifera L. seeds against CCl4-induced hepatotoxicity in rats. *Journal of ethnopharmacology*, *155*(1), pp.736-743. https://doi.org/10.1016/j.jep.2014.06.026

63. Dranoff, G., 2004. Cytokines in cancer pathogenesis and cancer therapy. *Nature Reviews Cancer*, *4*(1), pp.11-22. https://doi.org/10.1038/nrc1252

64. Coussens, L.M. and Werb, Z., 2002. Inflammation and cancer. *Nature*, *420*(6917), pp.860-867. https://doi.org/10.1038/nature01322

65. Loeppky, R.N., 1994. Nitrosamine and N-nitroso compound chemistry and biochemistry: advances and perspectives. https://doi.org/10.1021/bk-1994-0553.ch001